

Photoemission investigation of the electronic structure of amorphous and crystalline $\text{Fe}_x\text{Zr}_{100-x}$ ($x = 25, 33, 91$)

H. Neddermeyer and Th. Paul

Institut für Experimentalphysik der Ruhr-Universität Bochum, D-4630 Bochum, Federal Republic of Germany

(Received 3 March 1987)

We have measured polycrystalline Fe, polycrystalline Zr, and $\text{Fe}_x\text{Zr}_{100-x}$ metallic glasses ($x = 25, 33, 91$) in the amorphous and crystalline state by means of uv photoemission and Auger electron spectroscopy. The results are analyzed in terms of the electronic density of states. The amorphous Fe-Zr samples show an increasing density of states at the Fermi level with increasing Fe content in agreement with calculations and specific-heat measurements.

I. INTRODUCTION

In the last years much attention has been paid to Zr-based metallic glasses and, in particular, to the system $\text{Fe}_x\text{Zr}_{100-x}$. By using the well-known melt-spinning technique, one is able to force $\text{Fe}_x\text{Zr}_{100-x}$ into the amorphous state in two different ranges of atomic concentrations, namely for $88 \leq x \leq 92$ (Ref. 1) and for $20 \leq x \leq 40$.² The physical properties are very different in both regimes. The Fe-rich glasses are ferromagnetic and show Invar-like behavior of some of their magnetic properties,^{3,4} while the Fe-poor glasses are superconductors for $x \leq 29$.² For $x \geq 40$ they are magnetically ordered and in the range $29 \leq x \leq 40$ neither superconducting nor magnetic order could be detected.²

In spite of the fact that these properties might be understood more satisfactorily by considering the density of electronic states $N(E)$ or the density of states at the Fermi level $N(E_F)$, up to now only one photoemission measurement of a Fe-Zr glass has been published to our knowledge⁵ (see also Refs. 6 and 7). Since the preparation of metallic glasses may not always lead to exactly the same samples due to different cleanliness of the components and other specific experimental conditions, a confirmation of the reported photoemission results seems to be useful. Moreover, a study of a metallic glass system in a certain range of concentrations allows the observation of systematic effects in the density of states and their relation to other physical properties. For example, the differences of the crystallization temperature are noticeable for the Fe-Zr glasses. For $\text{Fe}_{91}\text{Zr}_9$ and $\text{Fe}_{20}\text{Zr}_{80}$ values of 500°C (Ref. 8) and 385°C (Ref. 9) were found, respectively. The influence of ordering on the electronic structure may be studied in the Fe-poor regime, where for $x = 33$ and 25, single-phase crystallization was observed¹⁰ and possible effects of ordering are therefore not obscured by multiphase crystallization.

In the present work we attempt to correlate the experimental electronic structure for the different concentration regimes with the physical behavior of this system. Our results from $\text{Fe}_{25}\text{Zr}_{75}$ will also be compared with a theoretical density of states.^{6,7} As experimental methods we used uv photoelectron (UPS) and Auger electron spectroscopy (AES). By means of the latter method, surface concentra-

tion of the components and contamination were determined as well as effects of charge transfer on alloying, which was examined by looking at the shape and position of the Fe $M_{2,3}VV$ Auger transitions.

II. EXPERIMENT

The apparatus used for the measurements consists of a main ultrahigh-vacuum (UHV) chamber with a base pressure of approximately 10^{-10} mbar, which contains an electron energy analyzer, a noble-gas-discharge lamp for generating uv line radiation and an electron gun for excitation of the Auger electrons. Via a gate valve the samples are transferable to the measuring position from a small preparation chamber, where the sample surfaces can be treated by Ar^+ or Ne^+ bombardment and heating. The energy distribution curves (EDC's) of the photoemitted electrons are measured with an energy resolution of better than 60 meV. They are corrected for the transmission function of the analyzer after a constant background has been subtracted from the raw data. The EDC's are plotted against the initial energy referring to the Fermi level $E_F = 0$. More details of the experimental setup have been described by Heimann *et al.*¹¹

We studied $\text{Fe}_x\text{Zr}_{100-x}$ ($x = 25, 33, 91$) and polycrystalline Fe (99.999% purity) and Zr (99.7% purity). The metallic glasses were prepared by melting the components of the same cleanliness in an Ar arc. After homogenizing them in high vacuum for 15 min at a temperature of 1250°C they were transformed into the amorphous ribbons by melt spinning. Although the above purity was the best one available for the present experiments, diffusion of bulk impurities to the surfaces caused some difficulties, as will be discussed below. The amorphous state of the ribbons was controlled by x-ray diffraction. Before mounting the samples in the preparation chamber, they were polished mechanically with diamond powder and electrolytically in a solution of 87 vol % CH_3CHOH and 13 vol % HClO_3 ($\text{Fe}_{33}\text{Zr}_{67}$ and $\text{Fe}_{25}\text{Zr}_{75}$) or 80 vol % $\text{CH}_3\text{CH}_2\text{OH}$ and 20 vol % HCl ($\text{Fe}_{91}\text{Zr}_9$). *In situ* cleaning was performed by bombardment with Ar^+ and finally with Ne^+ of 500-eV energy and heating in the case of the amorphous samples well below the crystallization temperature.

To crystallize the samples they were annealed at 500°C

for several hours. Single-phase crystallization of $\text{Fe}_{25}\text{Zr}_{75}$ and $\text{Fe}_{33}\text{Zr}_{67}$ (Ref. 9) was confirmed by x-ray diffraction after the photoemission measurements. Our ordered $\text{Fe}_{91}\text{Zr}_9$ sample contained three crystalline phases (α -Fe, Fe_3Zr , and Fe_2Zr) in agreement with previous results.⁸

Surface concentration of the constituents was controlled by measuring the Fe $M_{2,3}VV$ (45 eV), Fe L_3VV (701 eV) and Zr $M_{4,5}N_1N_1$ (145 eV) Auger transitions. The intensity ratio of the Fe and Zr peaks closely followed the bulk concentration of the constituents. The intensity ratio did not show changes after crystallization, which means that segregation effects of one component may be neglected. However, annealing to 500°C always produced appreciable surface contamination with C and O, which had to be removed by subsequent bombardment-heating cycles. Although every metallic glass sample was exposed to more than 30 bombardment cycles, the final surfaces (except for Zr) still showed a small residual contamination in the order of several percent of a monolayer.

Cleaning of Zr turned out to be especially difficult. After the first heating to temperatures at a few 100°C the EDC's essentially contained contributions from a thick oxide layer, the Fermi edge was then not visible. We estimate the contamination of the finally measured Zr sample to be in the order of one monolayer. The difficulty of cleaning the metallic glass samples and of keeping them clean was certainly related to the Zr content and its high reactivity. In order to be sure that the shape of the valence bands was not influenced by the residual contamination, a controlled adsorption of O_2 on $\text{Fe}_{91}\text{Zr}_9$ up to an exposure of 50×10^{-10} mbar s was performed. The relevant results are mentioned in Sec. III.

III. RESULTS

In Fig. 1 results from the amorphous (*a*) and crystallized (*c*) Fe-Zr glasses are shown as solid and dashed lines, respectively. The EDC's consist of a main peak (*A*) between -2 eV and E_F , whose detailed shape will be discussed below, and some additional features below -2 eV (*a*, *b*, *c*, and *B*). These additional structures, which are superimposed on a background of inelastically scattered electrons, appear with considerable intensity and are mostly an indication of the fact that the surfaces were contaminated to some extent. The presence of O is visible by the peaks observed at -5 eV (*a*) and -6 eV (*b*) for $x=91$, 33, and 25, respectively. Satellite emission from a two-hole bound state¹² may also contribute to the energy region at -6 eV. C contamination is associated with a small structure at -3 eV (*c*) and is only seen distinctly for crystallized $\text{Fe}_{25}\text{Zr}_{75}$. At -4 eV a peak (*B*) is found for $\text{Fe}_{33}\text{Zr}_{67}$ and $\text{Fe}_{25}\text{Zr}_{75}$, which could not be related to surface contamination and is therefore explained by a density-of-states feature of these materials. Our identification of the peaks associated with adsorbed species is based on AES measurements of samples with different amounts of surface contamination in the course of the preparation procedure.

The main structure (*A*) of the EDC's, i.e., the energy region between -2 eV and E_F , shows systematic effects with concentration. The most important observation is

the increase in the intensity for the amorphous samples immediately below E_F with increasing Fe content. For $x=91$ the maximum of the EDC lies directly below E_F , which means that the Fermi level is located in a rising part or at the maximum of the density of states. For $x=33$ and 25 the maximum of the EDC's lies 0.8 eV below E_F , and $N(E_F)$ is therefore smaller than for $x=91$. There is even a little difference between $x=33$ and 25. A second systematic effect is an increasing broadening of the whole high-energy structure (*A*) with decreasing Fe content. That the EDC's reflect properties of the density of states was confirmed by measuring at different photon energies ($\hbar\omega=16.85$ eV and in some cases also $\hbar\omega=11.83$ eV). Within the accuracy of the data no systematic changes of *A* with photon energy could be observed.

For an estimation of the general trend of $N(E_F)$ with the Fe concentration, the flat part of the EDC's directly below the Fermi level was approximated by straight lines (dashed-dotted lines in Fig. 1). Their height at E_F (indicated by the solid circles) may be used as qualitative measure for $N(E_F)$ and their position confirms the small decrease of $N(E_F)$ with Fe concentration. The effects of the small residual surface contamination on the shape of the EDC's in the vicinity of E_F was found negligible. Adsorption of O_2 on $\text{Fe}_{91}\text{Zr}_9$ and measurements on surfaces with heavy contamination showed that structure *A* is only

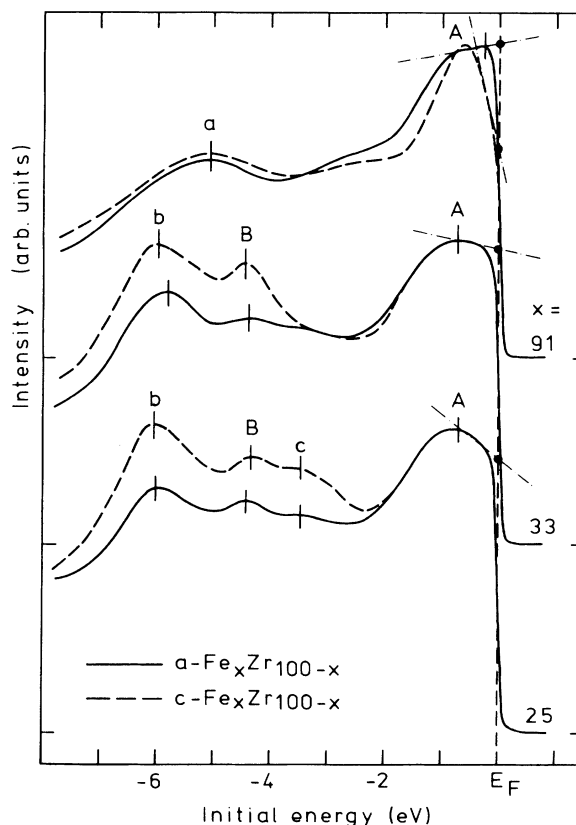


FIG. 1. Photoemission ($\hbar\omega=21.22$ eV) from amorphous (*a*-) and crystallized (*c*-) $\text{Fe}_x\text{Zr}_{100-x}$ ($x=25, 33, 91$).

influenced, when the contamination peaks *a*, *b*, and *c* have an intensity, which is comparable or larger than that of *A*. This is certainly not the case for the results presented in Fig. 1.

On crystallization of the samples the high-energy structure *A* does not show differences compared to the amorphous state for the ribbons with $x=33$ and 25. For $x=91$ a large effect is found, it appears as a reduction of the density of states at E_F . The latter observation may be related to the precipitation of α -Fe. A similarity of the EDC from c -Fe₉₁Zr₉ with that of c -Fe (see Fig. 2) is obvious. Differences in the low-energy region may be explained by an increased surface concentration of impurities for the annealed samples (in particular for Fe₂₅Zr₇₅). The overall agreement of the high-energy parts of the EDC's from the Fe-Zr samples with those of c -Fe and c -Zr (see Fig. 2) makes it plausible that they reflect the *d*-electron contributions of the constituents.

In Fig. 2 a comparison is made between our EDC's from a -Fe₂₅Zr₇₅, c -Fe, and c -Zr and published results from a -Fe₂₄Zr₇₆.⁵ The agreement between the experimental EDC's from the Fe-Zr glasses is fairly good. Small differences exist at E_F , which may be explained by a different energy resolution of the instruments, and in the low-energy region, which may be related to a different amount of surface contamination and, eventually, to a different background subtraction. For c -Zr only the high-energy region is shown. The low-energy part is dominated by emission from the O layer. The energy position of the maxima of the contamination peaks observed on c -Zr is indicated by the vertical bars (labeled *b* and *c*). We believe that structure *B*, which is not seen for Fe₉₁Zr₉ and Fe, may be assigned to emission from Zr states. It should be mentioned that $N(E_F)$ of the Fe-Zr glasses is remarkably higher than $N(E_F)$ of Fe. The intensity of the EDC from Zr at E_F may be influenced by the O layer.

Since for the metallic glasses our uv line source has been operated under the same conditions, it is possible to compare their photoemission intensity provided the surface quality of the samples is not too different. We might

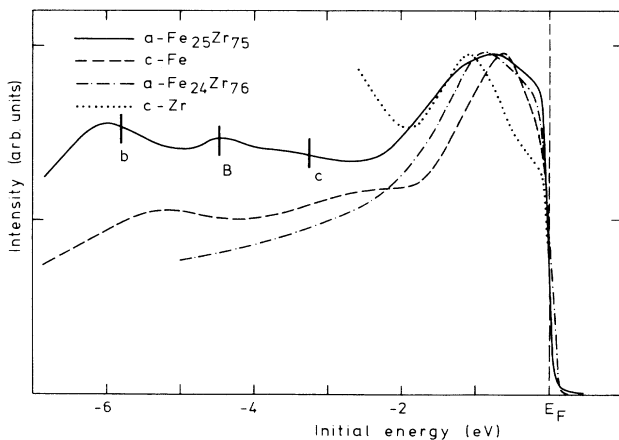


FIG. 2. Photoemission ($\hbar\omega=21.22$ eV) from a -Fe₂₅Zr₇₅, c -Fe, c -Zr, and a -Fe₂₄Zr₇₆ (Ref. 5).

then estimate the relative contributions to the EDC's from the Fe and Zr atoms. Since the free-electron-like *sp* electrons occupy a relatively broad band of states and therefore cannot contribute appreciably to the maximum of the EDC's, our estimation is essentially valid for the occupied *d* states. Experimentally we found that the intensity at the maximum is smaller by a factor of 0.4 for Fe₃₃Zr₆₇ and of 0.3 for Fe₂₅Zr₇₅ compared to emission from Fe₉₁Zr₉. If we use the atomic values for the number of *d* electrons at Fe and Zr sites (6 and 2, respectively), we may roughly evaluate the relative photoionization cross section for the Fe 3*d* and Zr 4*d* electrons. Effects of charge transfer and of changes of $N(E)$ with x are ignored by this procedure. At a photon energy $\hbar\omega=21.22$ eV, we estimated the cross section per electron for the Zr 4*d* electrons to be at least a factor of 5 smaller than for the Fe 3*d* electrons, which means that, e.g., for Fe₂₅Zr₇₅ the contribution to the EDC from the Zr 4*d* partial density of states is only in the order of 20% and for Fe₉₁Zr₉ 2% and therefore negligible for the latter material.

The work function of the samples was determined from the known energy difference between E_F and the low-energy photoemission threshold. For the various samples we found the following data: c -Zr (3.5 eV), a -Fe₂₅Zr₇₅ (3.61 eV), c -Fe₂₅Zr₇₅ (3.63 eV), a -Fe₃₃Zr₆₇ (3.59 eV), c -Fe₃₃Zr₆₇ (3.58 eV), a -Fe₉₁Zr₉ (4.39 eV), sputtered c -Fe₉₁Zr₉ (4.85 eV), annealed c -Fe₉₁Zr₉ (4.13 eV), and c -Fe (4.91 eV). The experimental error is 0.05 eV except for Zr, where the work function might be smaller by several 0.1 eV due to the non-negligible surface contamination. For Zr we made the observation that surface contamination always led to an increase of the work function. The work function of the Fe-Zr samples did not change on the crystallization for $x=25$ and 33, which is an indication of the same chemical constitution for the surfaces in the amorphous and crystalline state. The large effect observed for $x=91$ may be explained by the precipitation of α -Fe, which is exposed to the vacuum on sputtering.

Finally, we attempted to locate the energy position of the Fe $M_{2,3}VV$ Auger transitions. For the maximum we found the following values: a -Fe₂₅Zr₇₅ (43.50 eV), a -Fe₃₃Zr₆₇ (43.60 eV), a -Fe₉₁Zr₉ (43.71 eV), and c -Fe (44.05 eV). A small systematic shift of the Fe $M_{2,3}$ level with decreasing Fe concentration towards smaller binding energies is suggestive.

IV. DISCUSSION

Moruzzi *et al.*⁷ have computed the density of states of crystalline fcc FeZr₃ in the AuCu₃ structure and compared it with a photoemission measurement of a -Fe₂₄Zr₇₆.⁵ They suggested that the essential features of the electronic structure of the glassy alloy may be explained by the band structure of the ordered material. Our measurements support their suggestion by additional arguments. We are reminded that our EDC of a -Fe₂₅Zr₇₅ shows features in the low-energy part, which are absent in the experimental data of Oelhaf *et al.*⁵ (Fig. 2). While the lower-most peak (*b*) at -6 eV was assigned to O emission structure, *B* at -4 eV could not be explained by emission from adsorbed atoms. Since this peak is absent

for the Fe-rich sample (see Fig. 1), we explain this structure by emission from Zr states. A comparison of our photoemission results with the calculated density of states (Fig. 3) indeed shows agreement of the observed feature *B* with a small peak at -4 eV in the theoretical curves, which is mainly related to the Zr partial density of states.

A second point to be noticed is the fact that the experimental EDC of $a\text{-Fe}_{25}\text{Zr}_{75}$ shows its maximum at -0.8 eV and has a falling slope towards E_F , while the total theoretical density of states is approximately constant below E_F . This observation may qualitatively be explained by the slopes of the partial density of states which is rising for Zr and falling for Fe. Since the photoionization cross section is larger for Fe than for Zr states, we see that the weighted sum of both should decrease towards E_F as is observed in the experiment.

For $\text{Fe}_{91}\text{Zr}_9$ no theoretical density of states has been published, so far. Waseda *et al.*¹ have shown by means of x-ray diffraction measurements that the atomic structure of Fe-rich Fe-Zr glasses mainly depends on the dense random packing of Fe atoms. It might therefore be useful to compare the EDC with the calculated density of states of amorphous Fe.¹³ The calculation shows that the unhybridized Fe 3*d* bands have their maximum density of states immediately at E_F , the consideration of 4*s* state hybridization moves the maximum to somewhat lower energies. This is consistent with our observation that the maximum of the EDC for $a\text{-Fe}_{91}\text{Zr}_9$ is located at E_F . It is quite obvious that on going to crystalline Fe a lowering of the total energy is achieved, which finds its expression in a lowered value for $N(E_F)$ for *c*-Fe, see Fig. 2.

A remarkable feature of our measurements is the fact that in the glassy alloys $N(E_F)$ increases with increasing Fe concentration. The opposite has been concluded from measurements of the magnetic susceptibility.² On the other hand, in the Fe-poor regime an increasing $N(E_F)$ with increasing Fe concentration has been deduced from specific-heat studies,¹⁴ although the unknown phonon-electron coupling constant and the non-negligible magnetic contribution to specific-heat values¹⁵ makes this conclusion somewhat uncertain.

The breakdown of superconductivity for concentrations of $x \geq 29$ is not related to a decrease of $N(E_F)$, according to our measurements, but could be explained by the increasing magnetic interaction of the Fe atoms.^{16,17} An increase of $N(E_F)$ with Fe content has recently been found theoretically by Xanthakis *et al.*¹⁸ for $x = 20$ and 30 and is therefore in agreement with the present data.

We did not attempt to determine quantitatively the center of gravity for the occupied part of the *d* electronic states. From the measurements it is apparent, however, that the width of the *d* band structure *A* increases with increasing Zr content of the glasses, see Fig. 1. From this observation it might be suggested that an electron transfer from Zr to Fe atoms takes place leading to an increase of

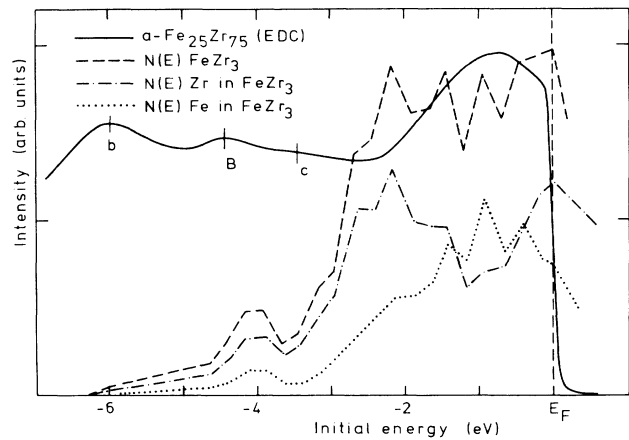


FIG. 3. Comparison between EDC from $a\text{-Fe}_{25}\text{Zr}_{75}$ and partial and total density of states from FeZr_3 calculated by Moruzzi *et al.* (Ref. 7).

the Fe and Zr *d* electron repulsion with increasing Zr concentration, which gives rise to a shift towards lower initial energies of the observed structure. This behavior may also qualitatively be deduced from the observed effects in the work function of the samples, where a systematic reduction with increasing Zr concentration was found.

V. CONCLUSION

The EDC's from amorphous and crystalline Fe-Zr alloys and those from crystalline Fe and Zr have been examined in terms of the density of electronic states. For all samples a peak near the Fermi level was observed, which has a basewidth in the order of 2 eV and was assigned to emission from the Fe 3*d* and Zr 4*d* electrons. By comparing the intensities of the EDC's the photoionization cross section of the Zr and Fe *d* electrons was estimated to be a factor of 5 smaller for the Zr 4*d* electrons in relation to that of the Fe 3*d* electrons. This means that the observed feature at E_F essentially reflects the behavior of the Fe *d* electrons. For the Fe-Zr samples an increasing density of states at E_F with increasing Fe concentration was obtained reaching a maximum value for $x = 91$. This behavior is in agreement with calculations and specific-heat measurements in the Zr-rich regime.

ACKNOWLEDGMENTS

This work has been supported by the Deutsche Forschungsgemeinschaft through funds of the Sonderforschungsbereich 166. We are grateful to Dr. M. Abd-Elmeguid and Dr. B. Wortmann who provided us with the metallic glass samples.

¹Y. Waseda, T. Masumoto, and S. Tamaki, *Proceedings of the Conference on Metallic Glasses, Science, and Technology*, edited by C. Hargitai, I. Bakonyi, and T. Kemény (Central Research Institute of Physics, Budapest, 1980), Vol. 1, p. 369.

²Z. Altounian and J. O. Strom-Olsen, *Phys. Rev. B* **27**, 4149 (1983).

³T. Masumoto, S. Ohnuma, K. Shirakawa, M. Nose, and K. Kobayashi, *J. Phys. (Paris) Colloq.* **C8**, 686 (1980).

⁴T. Kaneko, K. Shirakawa, S. Ohnuma, M. Nose, H. Fujimori,

- and T. Masumoto, *J. Appl. Phys.* **52**, 1826 (1981).
- ⁵P. Oelhafen, E. Hauser, and H.-J. Güntherodt, *Solid State Commun.* **35**, 1017 (1980).
- ⁶J. Kübler, K. H. Bennemann, R. Lapka, F. Rösel, P. Oelhafen, and H.-J. Güntherodt, *Phys. Rev. B* **23**, 5176 (1981).
- ⁷V. L. Moruzzi, P. Oelhafen, A. R. Williams, R. Lapka, H.-J. Güntherodt, and J. Kübler, *Phys. Rev. B* **27**, 2049 (1983).
- ⁸M. Sostarich and Y. Khan, *Z. Metallk.* **73**, 706 (1982).
- ⁹K. H. J. Buschow, I. Vincze, and F. van der Woude, *J. Non-Cryst. Solids* **53**, 101 (1983).
- ¹⁰I. Vincze, F. van der Woude, and M. G. Scott, *Solid State Commun.* **37**, 567 (1981).
- ¹¹P. Heimann, J. Hermanson, H. Miosga, and H. Neddermeyer, *Phys. Rev. B* **20**, 3059 (1979).
- ¹²L. A. Feldkamp and L. C. Davis, *Phys. Rev. Lett.* **43**, 151 (1979).
- ¹³T. Fujiwara, *J. Phys. F* **12**, 661 (1982).
- ¹⁴D. G. Onn, L. C. Wang, and Y. Fukamichi, *Solid State Commun.* **47**, 479 (1983).
- ¹⁵Y. Obi, L. C. Wang, R. Motsay, and D. G. Onn, *J. Appl. Phys.* **53**, 2304 (1982).
- ¹⁶M. Tenhover and W. L. Johnson, *Phys. Rev. B* **27**, 1610 (1983).
- ¹⁷M. Tenhover and D. Lukco, *J. Non-Cryst. Solids* **61-62**, 1049 (1984).
- ¹⁸J. P. Xanthakis, R. L. Jacobs, and E. Babič, *J. Phys. F* **16**, 323 (1986).